ISSUE: March 2013

Simplified Analysis Of A DCM Boost Converter Driving An LED String

Part II: Practical Considerations

by Christophe Basso, ON Semiconductor, Toulouse, France and Alain Laprade, ON Semiconductor, East Greenwich, R.I.

Part I of this article was dedicated to the theoretical analysis of a boost converter driving an LED string. This study was motivated by the need to stabilize the loop of an LED backlight driver in an automotive application. As pulse width modulation (PWM) is implemented for dimming control, loop control represents an important design consideration that conditions the final performance of the driver. In Part II, we describe the implemented solution and verify the measured frequency response versus the theoretical derivation from Part I.

The Electrical Schematic

Analog dimming of high-brightness white LEDs results in color shifting. In contrast, PWM digital dimming control prevents color shift as the luminous intensity produced by this method is that of the average lumens, while LED current amplitude during the PWM on-cycle is independent of the dimming ratio. Consequently, PWM-based control is generally the preferred dimming method.

Fig. 1 represents an LED driver for an automotive application where quiescent current is to be less than 10 µA when disabled. It features an NCV887300[1] ON Semiconductor 1-MHz nonsynchronous boost controller operating in constant-frequency discontinuous peak-current mode. The load consists of a string of 10 Nichia NSSW157-AT[2] white high-brightness LEDs. The corresponding board is shown in Fig. 2.

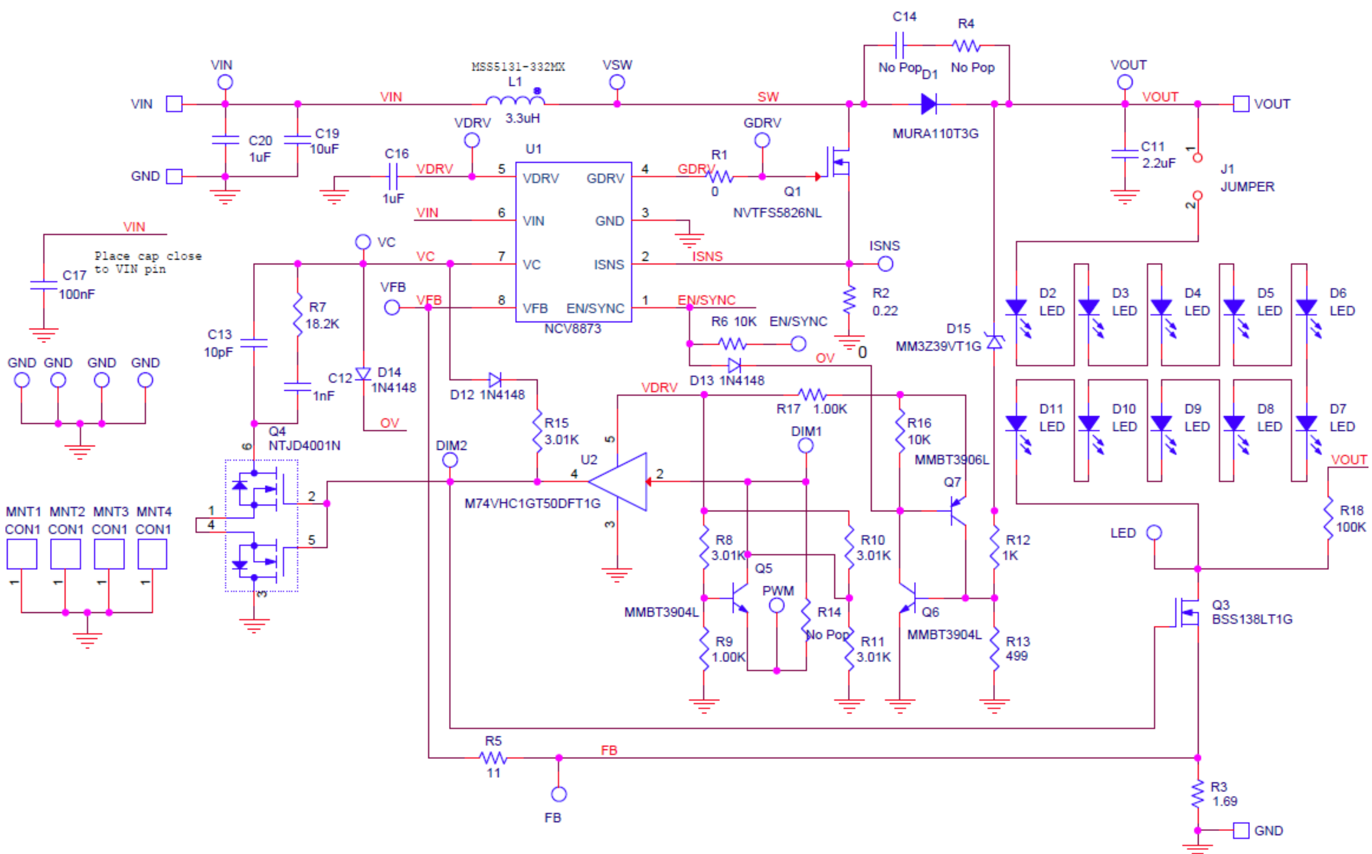

Fig. 1. Implementation of an LED driver with PWM dimming control based on the NCV887300 boost controller.

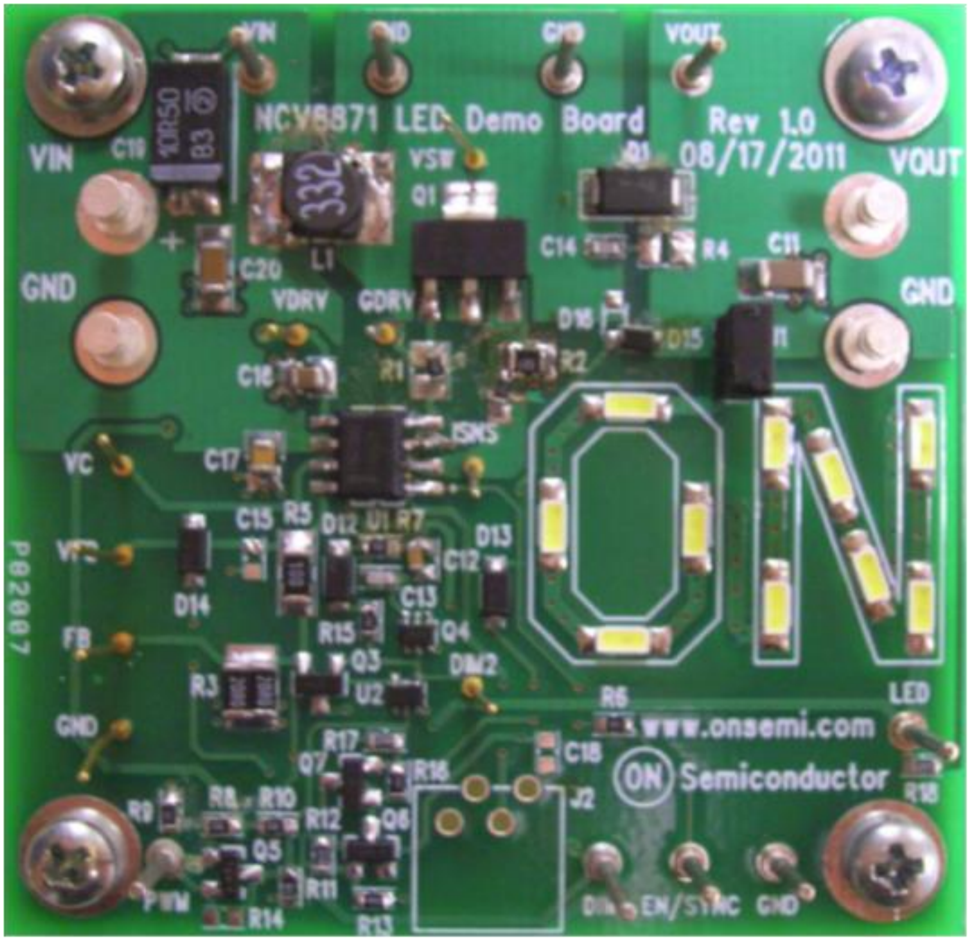

Fig. 2. Demonstration board for the dimmable LED driver circuit shown in Fig. 1.

For analysis of the LED driver circuit, there are five key parameters of the NCV887300 controller that must be noted.

- Quiescent current (I_q) < 6 µA (-40°C < T_J < 125°C) at V_{IN} = 13.2 V.
- EN/SYNC: facilitates interface to an external TTL enable command. The pin has a dual function also permitting oscillator synchronization to an external clock.
- ISNS: the boost transistor current-sense limit threshold voltage is 400 mV; internal slope compensation is 130 mV/µs.
- VC: internal operational transconductance amplifier (OTA) compensation pin. There is a die-level 542-Ω ESD series-protection resistor located between package pin and the amplifier output. Typical transconductance g_m is 1.2 mS. The OTA is 100 µA sink/source capable.
- VFB: LED current-sense resistor R3 is to be scaled based on an internal reference of 200 mV.

Design objectives and details of circuit operation for the Fig. 1 LED driver circuit are described in the following sections.

Design Objective

The circuit is capable of a PWM dimming ratio of 1000:1 for a 200-Hz PWM rate and an input voltage operating range of 6 V to 18 V. The resulting minimum pulse width calculates to 5 µs. The 1-MHz NCV887300 can generate a minimum of five boost-transistor gate pulses to maintain output capacitor charge for the LED current. A discontinuous-conduction-mode (DCM) boost topology is necessary to maintain voltage regulation, as the entire boost inductor energy is delivered after each gate pulse. A continuous-conduction-mode (CCM) topology would result in poor voltage regulation and undesirable analog dimming due to an energy build-up inertia in the boost inductor requiring several operating cycles.

Output-current leakage losses must be minimized to help maintain the output capacitor charge during deep dimming operation. Leakage current energy discharge results in partial-output-voltage discharge during the LED PWM off-time, which in turn, results in analog current dimming and a compensation network having a significant error when PWM on-time resumes. In practice, the need to minimize leakage influences several circuit design choices.

- Schottky rectifiers suffer from significant temperature-dependent leakage current. To minimize the boost-rectifier leakage current, an ultrafast technology boost rectifier was chosen in the Fig. 1 circuit.

- Ceramic capacitors have significantly less leakage current than electrolytic capacitors and are preferred as output boost capacitors.

- The current draw of the output-overvoltage monitoring circuit must be kept to a minimum. Monitoring circuits making use of resistor divider networks to ground are ill-suited for this purpose. A Zener-activated overvoltage detection circuit was selected because the Zener knee voltage is significantly higher than the battery voltage and leakage current is extremely low.

Circuit Operation

Q3 interrupts the digital current flow for PWM digital dimming control. When the PWM command is active low, D12 clamps the IC VFB feedback control voltage to a value below that of the controller regulation point and interrupts the booster IC GDRV FET gate drive signal. Q4 serves as a compensation network state sample/hold function for deep-dimming applications. By disconnecting the compensation network during PWM dimming, feedback compensation capacitor charge (C12 and C13) are maintained and rapid dynamic control resumes when the PWM command becomes active high.

Q5 together with R8/R9/R10/R11 are used for level shifting of the 1.8-V logic PWM dimming signal. U2 buffers the PWM signal to drive the bidirectional switch Q4.

If left undetected, an open-LED failure event would result in an overvoltage operating condition. Current-sense resistor R3 voltage feedback would be 0 V and an open-loop output overvoltage condition would result. Discrete passive components were selected to implement the overvoltage protection function to minimize output leakage current losses when the LED system is externally disabled. Zener diode D15 conduction senses the overvoltage condition, initiating a controller IC softstart (D13) by pulling the enable pin low, interrupting boost voltage switching operation (D14). Resistor R18 provides a discharge path for output boost energy storage capacitor C11.

Removal of jumper J1 disables the LED chain to permit connecting an external load between the VOUT terminal and the LED terminal.

Resistor R5 is an injection point for a frequency-response analyzer across terminals VFB and FB. Its presence does not influence the system loop response. By injecting a frequency-response analyzer signal across R5, the control-output (FB/VC terminals), amplifier (VC/VFB) and open-loop-gain-in-closed-loop-form (FB/VFB) responses may be measured.

Characterizing The LED AC Dynamic Resistance

The LED dynamic resistance may be approximated from characterization curves found in manufacturer datasheets measured under specific operating conditions. The system-specific thermal operating conditions may be very different. In Part I, a system-level method of measuring LED dynamic resistance that characterizes the device under system-level thermal conditions was described. For this article, a frequency-response analyzer was used to measure the in-circuit value of the current-sense resistor, the PWM FET resistance and the cumulative series dynamic resistance under thermally stable operating conditions at 100% PWM duty ratio (Fig. 3.)

Closed-Loop Analysis

A control-output (V_{out}) expression $H(s)$ was derived in Part 1 of this article. Power is delivered to the LED string, however the feedback control feedback term is that of the LED current-sense resistor voltage V_{sense} (Fig. 4.) The plant transfer function $H(s)$ must be scaled accordingly per expression (1) below.

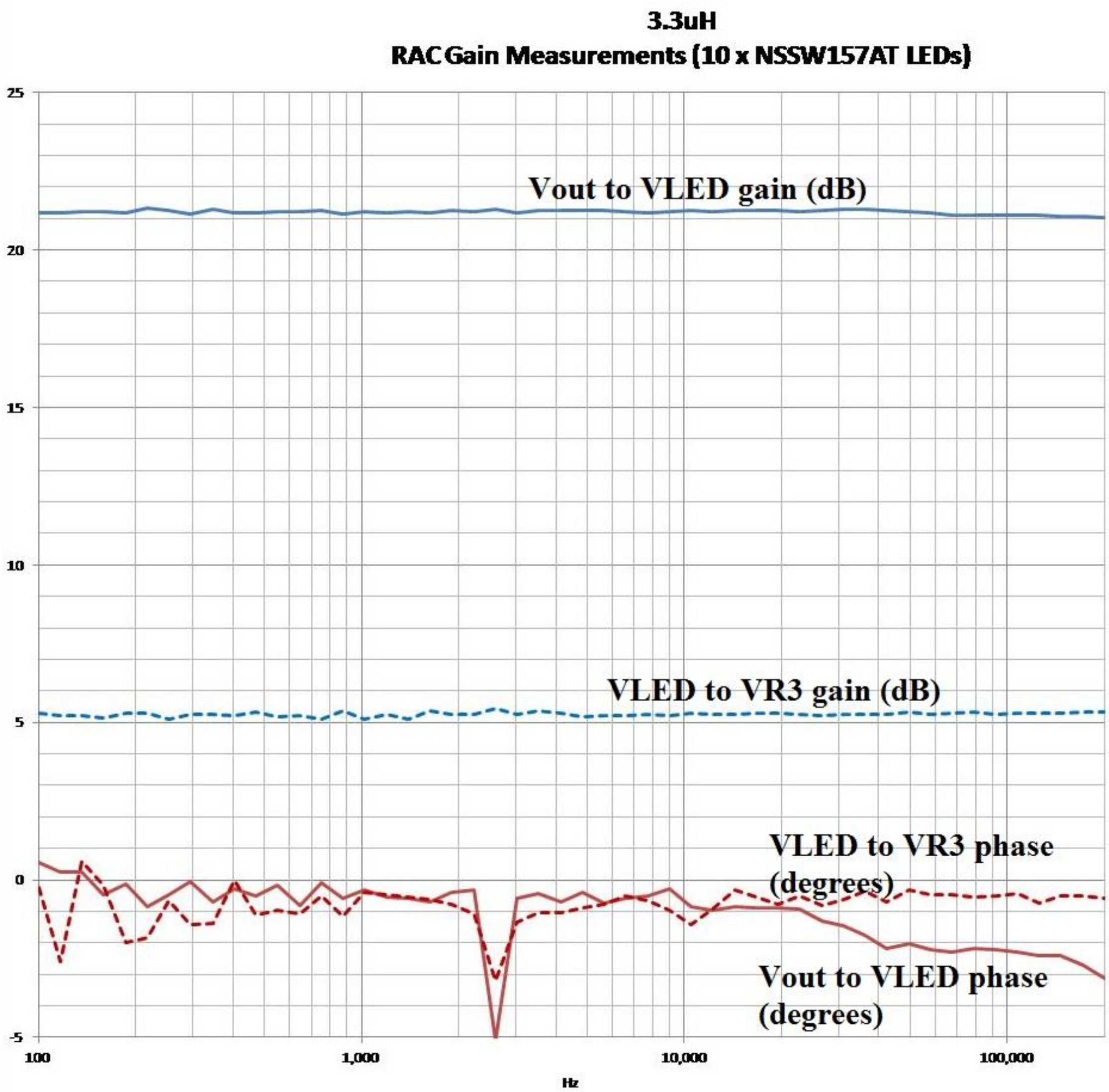

Fig. 3. In-circuit small signal response for the current-sense feedback network.

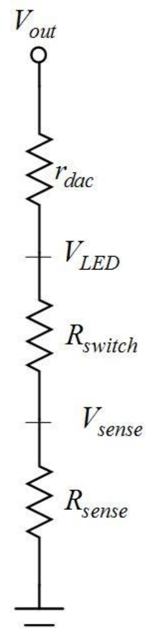

Fig. 4. Current-sense feedback.

$$H_c(s) = \frac{R_{sense}}{R_{ac}} H_0 \frac{1+\frac{s}{\omega_z}}{1+\frac{s}{\omega_p}} \tag{1}$$

where

$$H_0 = \frac{V_{in}{}^2 V_c L}{T_{sw}(V_{out} - V_{in})(S_e L + R_i V_{in})^2} R_{eq}, \tag{2}$$

$$R_1 = \frac{2T_{sw}(V_{in} - V_{out})^2 (S_e L + R_i V_{in})^2}{V_c{}^2 V_{in}{}^2 L}, \tag{3}$$

$$R_{ac} = R_{dac} + R_{switch} + R_{sense}, \tag{4}$$

$$R_{eq} = \frac{R_1 R_{ac}}{R_1 + R_{ac}}, \tag{5}$$

$$\omega_z = \frac{1}{r_C C_{out}} \text{ and} \tag{6}$$

$$\omega_p = \frac{1}{(r_C + R_{eq}) C_{out}}. \tag{7}$$

Vc may be obtained from (8).

$$D = \frac{V_c L}{S_e T_{sw} L + R_i T_{sw} V_{in}} \tag{8}$$

The parameters for the LED dynamic resistance, series PWM transistor and current-sense resistor were measured under thermally stable system-level operating conditions. The main operating parameters were V_{IN} = 12 V and I_{out} = 116 mA. Measured open-loop response $H_c(s)$ is plotted along with calculated results in Fig. 5. Table 1 lists the measured parameters used for the calculations for the Fig. 1 schematic.

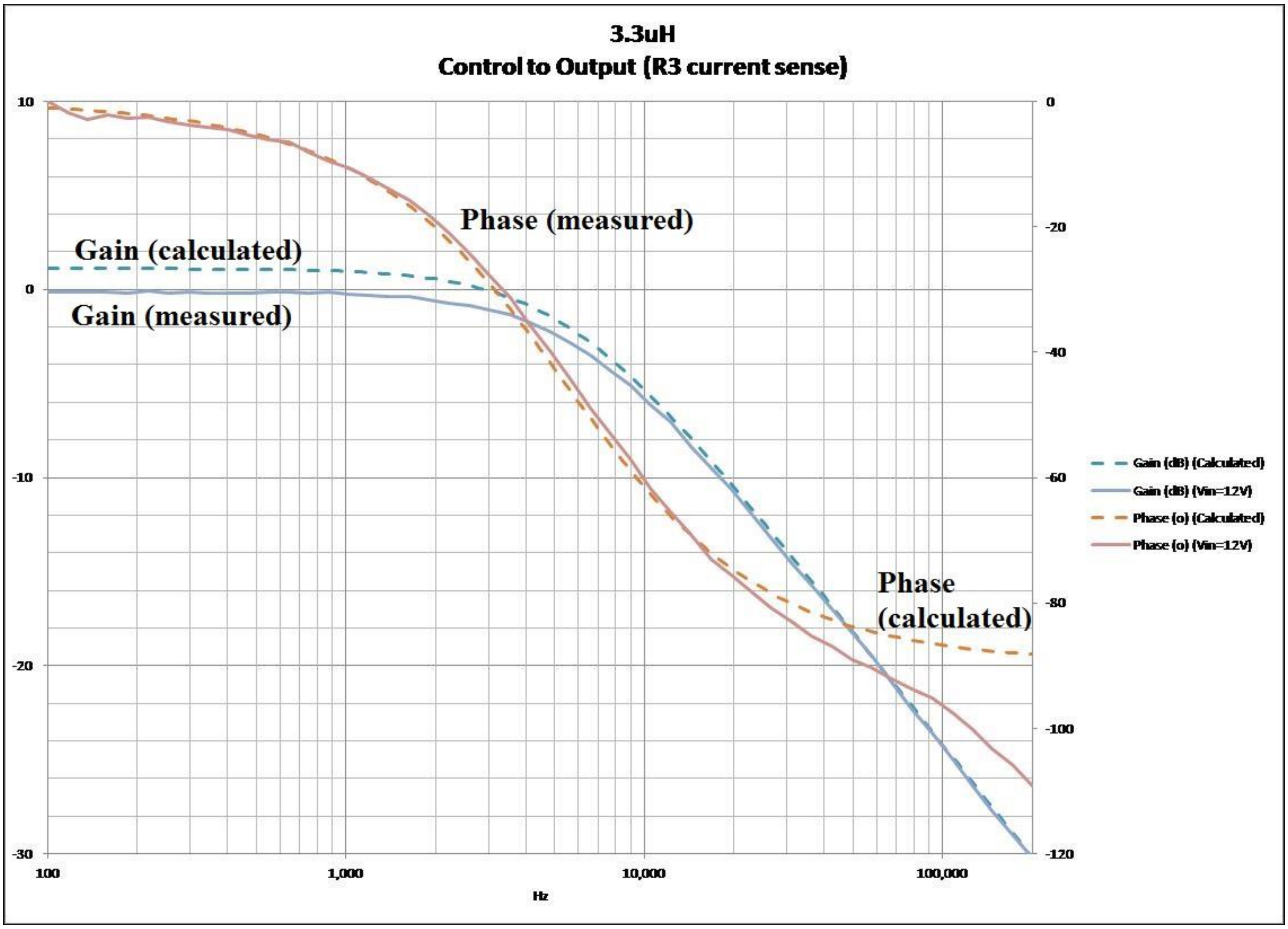

Fig. 5. Control-to-output response—measured versus calculated results.

Table 1. Demo board circuit parameters

Parameter	Data	Note
r_{LED} (10 LED chain)	33.1 Ω	Measured
R_{switch} (Q3)	1.44 Ω	Measured
R_{sense} (R3)	1.73 Ω	Measured
V_{OUT}	29.75 V	Measured
V_{IN}	12.0 V	Measured
R_i	0.22 Ω	
S_e	130 mV/µs	
C_{out}	1.0 µF	GRM31CR71H225KA88L dc-biased and temperature-adjusted
r_c	4 mΩ	
I_{out}	116 mA	Measured
L	3.3 µH	MSS5131-332MX
LED load	NSSW157AT	10-LED chain
T_{sw}	1 µs	

A difference between theoretical and empirical phase measurements becomes apparent at high frequency. The discrepancy is attributed to the missing RHPZ term from the numerator of the modulator transfer function in expression (1), which was described as a limitation of the simplified calculation derivation in part I of this article.[4]

A small difference (~1 dB) between low-frequency gain theoretical and measured results is observed. Operating losses from the boost inductor, transistor and rectifier were neglected in the derivation of the dc operating point. If such losses were considered, the duty ratio dc operating point would be slightly larger, resulting in a reduction of the low-frequency gain. This can be observed by modifying V_{in} (reduced to emulate resistive losses) and V_{out} (increased to include the boost-diode voltage drop) terms in expression (2).

System Performance

Operating waveforms for the LED dimming circuit from Fig. 1 configured for 1000:1 200-Hz PWM dimming are shown in Fig. 6. There is a slight voltage discharge of the compensation capacitor that is visible on the VC waveform and this results from a race condition between bidirectional switch Q4 response time and the PWM clamp activation via D12. R15 is introduced in series with clamp diode D12 to limit compensation network charge depletion. Waveform VFB maintains the desired digital wave shape and amplitude (no analog dimming.)

The extra short duration GDRV waveform (sixth pulse) occurring after the PWM signal command goes to a low state is a result of the NCV887300 internal logic propagation delay response time. The energy from this extra pulse is beneficial to help maintain charge in the output boost capacitor as it compensates for some parasitic leakage energy losses during deep PWM dimming operating mode.

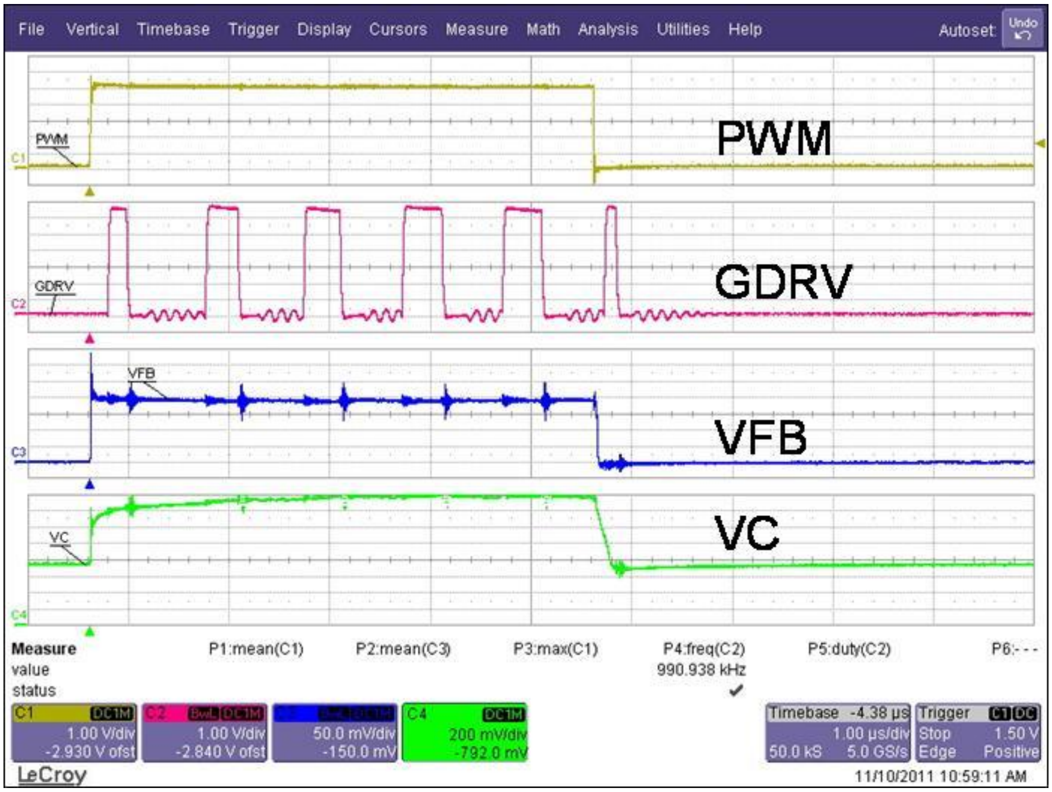

Fig. 6. 1000:1 200-Hz deep dimming operation.

Conclusion

The expressions derived in Part I of this article for the theoretical small-signal response for a DCM boost converter driving an LED string were successfully applied in the analysis of an LED PWM dimming circuit. The practical aspects of implementing this dimming circuit with the capability of 200-Hz 1000:1 deep dimming were discussed. Simulation and measurement results were found to correlate with the exception of a phase error that appears at high frequency due to the missing RHP zero in the theoretical expression. Waveforms measured at 1000:1 200-Hz PWM operation demonstrated very good operating performance.

References

1. ON Semiconductor NCV887300 Automotive Grade Non-Synchronous Boost Controller Datasheet, www.onsemi.com/PowerSolutions/product.do?id=NCV8873.

2. Nichia Corporation NSSW157AT White LED Datasheet, http://www.nichia.co.jp/en/product/led.html#.

3. "Switch Mode Power Supplies: SPICE Simulations and Practical Designs," by Christophe Basso, McGraw-Hill 2008, ISBN 978-0-07-150859-9.

4. "Simplified Analysis of a DCM Boost Converter Driving an LED String, Part I: Theoretical Analysis," by Christophe Basso and Alain Laprade, How2Power Today, February 2013.

About The Authors

Christophe Basso is an application engineering director at ON Semiconductor in Toulouse, France. He has originated numerous integrated circuits among which the NCP120X series has set new standards for low standby power converters. SPICE simulation is also one of his favorite subjects and he has authored two books on the subject. Christophe's latest work is "Designing Control Loops for Linear and Switching Power Supplies: A Tutorial Guide."

Christophe received a BSEE-equivalent from the Montpellier University, France and an MSEE from the Institut National Polytechnique de Toulouse, France. He holds 17 patents on power conversion and often publishes papers in conferences and trade magazines.

Alain Laprade received an MEng in electrical engineering from McGill University in Montréal in 1984. Since then he has worked in power supply development for commercial, telecommunication, automotive, and aerospace applications as an applications engineer. In 2010, he relocated to Rhode Island to join ON Semiconductor's Analog Power Group New Product Development team.

For further reading on the design of LED drivers, see the How2Power Design Guide, select the Advanced Search option, go to Search by Design Guide Category and select "LED Lighting" in the Popular Topics category.